EUROPEAN JOURNAL OF MATERIALS SCIENCE AND ENGINEERING
Volume 10, Issue 3, 2025: 225-234 | www.ejmse.ro | ISSN: 2537-4338

EJMSE

DOI: 10.36868/ejmse.2025.10.03.225

ELECTROCHEMICAL BEHAVIOR OF NEW BIOCOMPATIBLE TITANIUM ALLOYS CONTAINING Mo, Zr, Ta, AND Nb

Madalina Simona BALTATU[1] [0000-0002-5278-8958], Andrei Victor SANDU[1,2,3] [0000-0002-9292-749X], Andrei PRUTEANU[1] [0009-0005-3483-3371], Dragos Cristian ACHITEI[1] [0000-0002-8562-9507], Manuela Cristina PERJU[1] [0000-0002-2718-2698], Dumitru Doru BURDUHOS-NERGIS[1] [0000-0002-2716-1328], Mirabela Georgiana MINCIUNA[1] [0000-0001-9523-4974], Petrica VIZUREANU[1,2,*] [0000-0002-3593-9400]

[1] "Gheorghe Asachi" Technical University of Iași, Faculty of Materials Science and Engineering, Iași, Romania
[2] Academy of Romanian Scientists, 54 Splaiul Independentei St., Sect. 5, 050094, Bucharest, Romania
[3] Romanian Inventors Forum, Str. Sf. P. Movila 3, Iasi, Romania

Abstract

Metallic implants operate in a complex physiological environment where electrochemical processes govern corrosion and long-term performance. This work investigates the electrochemical behavior of pure titanium, molybdenum, zirconium, tantalum, and niobium in Ringer's solution at pH 5.5, using linear polarization, cyclic polarization, and electrochemical impedance spectroscopy (EIS). The results show that titanium and tantalum rapidly form compact and adherent oxide films (TiO_2, Ta_2O_5), which ensure passivation and low corrosion rates. Zirconium exhibits limited passivation with porous oxide layers and mainly generalized corrosion, while molybdenum does not form a stable passive film and corrodes actively, producing weakly adherent porous oxides. Niobium displays intermediate behavior, with partial passivation but reduced stability compared to Ti and Ta. The EIS spectra were adequately fitted using equivalent circuit models with two time constants and constant phase elements. These findings provide a reference framework for understanding the individual role of each element in designing and optimizing future Ti–Mo–Zr–Ta–Nb biomedical alloys.

Keywords: *titanium, niobium, tantalum, Ringer's solution, polarization, EIS, CPE, obtaining.*

Introduction

Biocompatible materials represent the class of materials capable of interacting with the biological environment without inducing significant adverse reactions and without compromising the functionality of surrounding tissues or organs. Among them, metallic biomaterials play a central role due to their high mechanical strength, chemical stability and the possibility of processing into complex shapes required for orthopedic, dental or cardiovascular implants [1-2]. In recent decades, titanium alloys have gained particular attention due to the unique combination of properties: low density, favorable strength-to-weight ratio, excellent biocompatibility and corrosion resistance in the physiological environment [3-5].

The corrosion resistance of titanium and its alloys is conferred by the spontaneous formation of a thin and adherent layer of titanium dioxide (TiO_2), which acts as a protective barrier on the surface of the material. However, the stability and characteristics of this passive layer are influenced by the chemical composition of the alloy, the microstructure of the material and the chemical-physical conditions of the biological environment. Metallic implants are permanently exposed to aqueous, compositionally complex biological fluids containing nutrients, organic species and electrolytes [4]. This aqueous nature makes electrochemical processes govern the corrosion mechanisms, and pH variations or the presence of aggressive agents can accelerate degradation [6-8]. Although body fluids are buffered at an average pH

*Corresponding author: peviz2002@yahoo.com

of 7.4, conditions such as infections or surgical interventions can cause significant deviations, modifying the corrosion behavior of implants [8-12].

In this context, the Ti–Mo–Zr–Ta–Nb system has emerged as a promising alloy system for biomedical applications, as it combines the advantages of titanium with the beneficial effects of alloying elements. Molybdenum, tantalum and niobium act as β-stabilizers, contributing to reducing the elastic modulus and improving mechanical compatibility with human bone, while zirconium and tantalum favor the formation of compact and protective passive films [13-15]. This synergy allows the production of alloys with increased corrosion resistance and superior biocompatibility, capable of meeting the stringent requirements of modern implants [16-17].

Although the present study focused on the electrochemical behavior of the pure constituent metals, the elaboration of Ti–Mo–Zr–Ta–Nb alloys by vacuum arc remelting establishes the experimental basis for future corrosion and biocompatibility investigations directly on multicomponent systems.

Materials and Methods

Obtaining alloys

The development and design of metallic materials used as biomaterials have involved a detailed analysis of both the design parameters and the technological conditions imposed by the manufacturing equipment. Although titanium-based alloys have high potential for numerous biomedical applications, production volumes remain low due to the high costs associated with conventional methods [14-17]. These costs are related to the processing temperatures, which frequently exceed 1600°C, values higher than those required for steels or aluminum alloys. In addition, molten titanium exhibits a very intense chemical reactivity with almost any material with which it comes into contact, which complicates the design of stable and economical crucibles. For this reason, current commercial technologies aim to avoid contact of the melt with other materials, resorting to vacuum arc remelting and the use of cold water-cooled crucibles [16-19].

The design of the new Ti–Mo–Zr–Ta–Nb alloys was based on the physical properties of the component elements, the analysis of binary equilibrium diagrams and on biocompatibility and corrosion resistance criteria. The basic properties of the alloying elements, such as melting temperature and density, are presented in Table 1, and the chemical compositions of the proposed alloys are summarized in Table 2.

Table 1. Physical properties of the alloying elements used

Element	Melting point (°C)	Density (kg/m³)
Ti	1668	4507
Mo	2625	10200
Zr	1855	6511
Ta	3020	16650
Nb	2477	8570

Table 2. Compositions of the proposed Ti–Mo–Zr–Ta–Nb alloys (% mass)

Ti (%)	Mo (%)	Zr (%)	Ta (%)	Nb (%)
53.0	20.0	7.0	15.0	5.0
51.0	20.0	7.0	15.0	7.0
48.0	20.0	7.0	15.0	10.0
43.0	20.0	7.0	15.0	15.0

Vacuum arc remelting installation

To obtain the alloys, a vacuum arc remelting installation was used, which includes a sealed chamber, a water-cooled copper crucible and a non-consumable mobile electrode made of thoria tungsten, connected to a direct current source capable of providing melting currents of the order

of hundreds of amperes. The electric arc is established between the electrode and the crucible nest, and the solidification film formed on the copper surface prevents direct contact between the melt and the crucible material. The installation allows for high temperatures to be reached, operation in a protective argon atmosphere after successive vacuum and purge stages, as well as permanent monitoring of the vacuum level. The construction facilitates rapid loading and unloading, and internal lighting ensures visual control of the melting bath [20-23].

The chosen method consisted of arc remelting in a protective atmosphere to ensure compositional homogeneity and the absence of inclusions. The raw materials had high purities (Ti 99.7%, Mo 99.5%, Zr 99.4%, Ta 99.3%, Nb 99.5%) and were prepared by degreasing and cutting to appropriate sizes. The loading into the crucible was carried out considering the differences in density and melting temperature, after which the chamber was evacuated to about 4.5×10^{-3} mbar and purged with argon in repeated cycles. The process was visually monitored, and six successive remeltings of each ingot were performed for homogenization. The ingots obtained provided sufficient material for the preparation of the specimens intended for testing.

Electrochemical methodology

The specimens had dimensions of 11 × 5 × 5 mm, were degreased in ethyl alcohol, washed in distilled water under ultrasonic agitation, and polished progressively up to 4000 grit. The corrosion medium consisted of Ringer's solution containing NaCl 8.6 g/L, KCl 0.3 g/L, and $CaCl_2$ 0.33 g/L, adjusted to pH 5.5. All measurements were carried out at 20 °C in naturally aerated solutions, with potentials referred to the saturated calomel electrode (SCE) and platinum used as the counter electrode.

Linear polarization tests were performed in the potential range −200 to +500 mV vs. OCP, at a scan rate of 0.5 mV/s. The parameters E_{cor}, R_p, j_{cor}, and v_{cor} were extracted from Evans diagrams in a ±60 mV interval around E_cor. Cyclic polarization measurements were conducted in the potential range −500 to +2000 mV and back to −500 mV, at a scan rate of 10 mV/s, in series of 6–8 consecutive cycles, determining E_{cor}, E_{rp}, and j_{2V}. Electrochemical impedance spectroscopy (EIS) was carried out at OCP, in the frequency range 10^5 to 2×10^{-2} Hz, with an amplitude of 10 mV. The impedance data were fitted using equivalent circuits with constant phase elements (CPEs) and, where appropriate, a Warburg diffusion element.

Results and Discussions

The determination of corrosion parameters based on linear and cyclic polarization allowed the evaluation of the individual behavior of each component metal of the Ti–Mo–Zr–Ta–Nb system, used in obtaining biomedical alloys. The data summarized in Table 3 and Table 4, corroborated with the comparative Evans diagram (Fig. 1), highlight major differences between the analyzed metals, differences that are reflected both in the corrosion mechanisms and in their passivation possibilities.

Table 3. Instantaneous corrosion parameters for the alloy components in Ringer's solution

Alloy	E_{cor} [mV]	R_p [kohm.cm^2]	J_{cor} [mA/cm^2]	v_{cor} [mm/an]	b_a [mV/dec.]	b_c [mV/dec.]
Titanium	-330	25.85	1.36	11.85	201	-204
Molybdenum	-83	1.21	19.05	165.5	97	-80
Zirconium	-367	7.83	3.02	34.46	100	-146
Tantalum	-324	9.00	3.57	25.33	150	-270
Niobium	-243	0.392	81.47	707.2	239	-159

Table 4. Corrosion parameters of pure metals obtained from cyclic polarization curves in Ringer solution

Alloy	E_{cor}, [mV]	E_{rp} [mV]	j_{2V} [mA/cm^2]	R_p [KΩ.cm^2]	j_{cor} [mA/cm^2]	v_{cor} [mm/an]
Titanium	-130	+126	0.344	17.51	1.943	16.93
Molybdenum	-159	+168	74.50	0.98	23.04	243.9
Zirconium	-372	+6,3	0.433	5.52	5.89	67.27
Tantalum	-288	+68	0.751	11.17	2.92	25.23
Niobium	-270	+60	0.721	10.23	2.85	24.20

Regarding the corrosion potential (E_{cor}), the recorded values are in the range −80…−370 mV, with titanium and zirconium having the most negative values, which indicates a more pronounced tendency for spontaneous oxidation. Molybdenum, on the other hand, has a nobler Ecor, but correlated with a much higher corrosion current density (jcor), which leads to a corrosion rate almost two orders of magnitude higher than in the case of titanium or tantalum. This aspect shows that the potential alone is not sufficient to characterize corrosion resistance, and simultaneous analysis of corrosion currents is necessary.

The corrosion current density (jcor) and the corrosion rate (vcor) are the critical parameters for assessing the behavior in physiological solution. Niobium and molybdenum presented the highest jcor values (over 20 mA/cm²), with extremely accelerated corrosion rates (over 200 mm/year), which gives them a low stability in the pure state (Table 3). In contrast, titanium and tantalum are distinguished by low jcor values (1–3 mA/cm²) and low corrosion rates (<30 mm/year), which confirms their role as stabilizing and passivating elements in alloy compositions. Zirconium occupies an intermediate position, with a corrosion rate of the order of tens of mm/year, but without consistent passivation, which limits its individual use.

Fig. 1 (comparative Evans diagram) clearly illustrates these behaviors. The anodic branches of titanium and tantalum move rapidly towards the passivation region, confirming the formation of compact protective films of TiO_2 and Ta_2O_5, which limit the propagation of the corrosion process. In contrast, molybdenum presents a steep anodic branch and the lack of a passivation plateau, indicating generalized corrosion, accompanied by the formation of unstable oxides (MoO_2, MoO_3) and soluble products (H_2MoO_4), which do not protect the surface. Zirconium is characterized by an almost perfect overlap of the anodic and cathodic branches at each cycle, which demonstrates an active corrosion process, without an effective protective barrier [19-20].

Cyclic polarization (Table 4) provides additional information on the stability of passive films. Titanium and tantalum show a significant decrease in current density at high potentials after the first cycles, which shows the consolidation of the protective film. For example, in the case of titanium, the current density at +2 V decreases from 344 mA/cm² to almost half (169 mA/cm²) after a few cycles, and for tantalum the decrease is from 751 mA/cm² to 412 mA/cm². This phenomenon indicates an increase in the thickness and density of the protective oxide layer with the repetition of electrochemical stresses. In contrast, zirconium and molybdenum do not show a similar behavior, j_2V remaining high or even increasing slightly, which confirms the porous and unstable nature of the oxides formed [23-25].

Polarization resistance (Rp) is another differentiating parameter. Titanium has the highest Rp values, followed by tantalum, which once again confirms the stability of these metals in Ringer's solution. Niobium, on the other hand, has very low values, reflecting its high susceptibility to corrosion.

Comparative analysis of linear polarization curves, cyclic voltammograms and electrochemical impedance spectra in Ringer solution shows that titanium and tantalum present the best passivation capacity, by forming compact protective films of TiO_2 and Ta_2O_5, respectively, which leads to low corrosion current densities and low degradation rates, as observed in Table 4 and in the way in which the anodic branches quickly enter the passive region in the Evans diagram in Fig. 1. As the process is repeated through successive cycles, the

consolidation of the passive films becomes evident: the current density at +2 V decreases significantly for Ti (from 344 to ~169 mA/cm²) and for Ta (from 751 to ~412 mA/cm²), confirming the progressive stabilization of the protective layer, a result visible in Table 4 and coherent with the difference between the forward and reverse branches in the voltammograms.

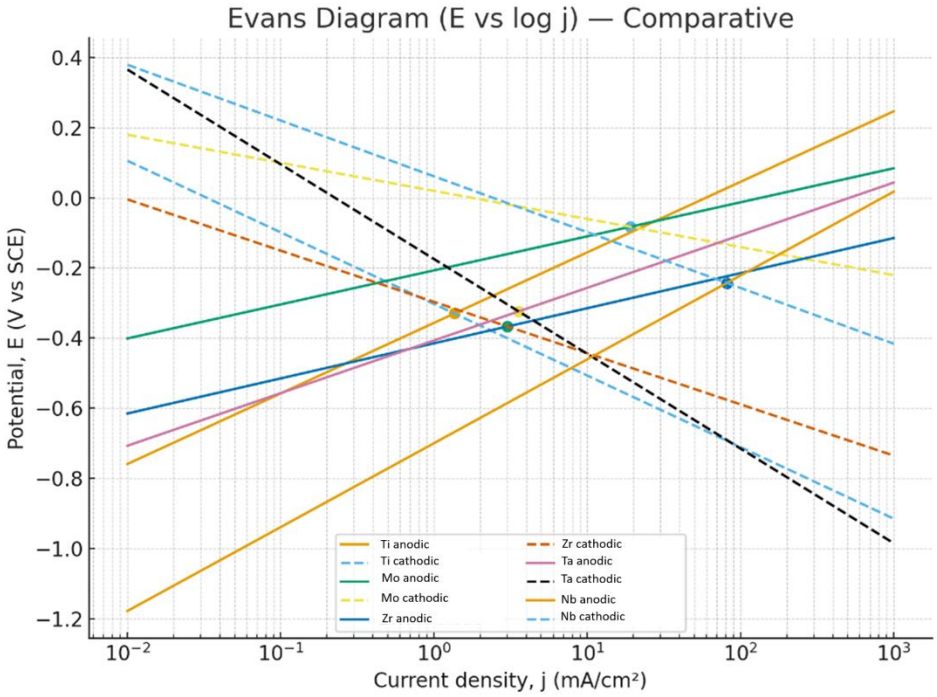

Fig. 1. Evans diagram constructed from Tafel extrapolation of polarization curves for pure metals (Ti, Mo, Zr, Ta, Nb) in Ringer's solution, showing anodic (solid lines) and cathodic (dashed lines) branches and the corresponding corrosion potentials (Ecor) and current densities (jcor)

In contrast, molybdenum does not exhibit effective passivation under the tested conditions; the high currents, the apparent increase in current density with the number of cycles, and the presence of a porous and non-protective corrosion product (MoO_2, with MoO_3 formation only in the trans-passive state and conversion to soluble H_2MoO_4) explain the high corrosion rate shown in Table 3 and the very high j_2V values in Table 4. Zirconium exhibits a weak passivation tendency, with the anodic and cathodic curves remaining almost superimposed from one cycle to the next, and the modest reduction in j_2V after several cycles indicates the formation of a porous, permissive layer. Niobium exhibits an intermediate behavior, without reaching the performance of Ti/Ta in terms of electrochemical protection.

The EIS results support this mechanistic picture: the modeling with equivalent circuits with two time constants and constant phase elements (Fig. 2) reveals non-ideal capacitances of the double layer and the passive film ($n<1$), while the values of the passive layer resistance and the charge transfer resistance clearly differentiate the systems. For titanium, the film is thin but stable; for tantalum, the passive film is thicker and very compact; for molybdenum, although the layer resistance may seem high, the porosity and low adhesion compromise the protection, which corresponds to the high polarization currents.

For a quantitative characterization of the electrochemical behavior, the experimental data obtained by impedance spectroscopy were fitted using the equivalent circuits presented

previously. The values of the extracted parameters for each model and for the pure metals in Ringer's solution are presented in Tables 5–7.

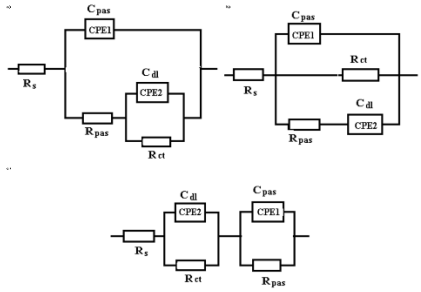

Fig. 2. Equivalent circuits used for fitting the Electrochemical Impedance Spectroscopy (EIS) data of Ti, Mo, Ta, Zr, and Nb in Ringer's solution: a) R(Q(R(QR))), b) R(QR(QR)), c) R(QR)(QR).

Table 5. Values of the equivalent circuit elements R(Q(R(QR))) for pure metals in Ringer's solution

Alloy	R_s Ohm.cm^2	CPE1 $10^4.Q_{pas}$ S.s^n/cm^2	n_1	R_{pas} Ohm.cm^2	CPE2 $10^4.Q_{dl}$ S.s^n/cm^2	n_2	R_{ct} Ohm.cm^2	$10^3.\chi^2$	ε (%)
Titanium	26.86	1.260	0.638	13.4	0.917	0.757	13730	0.796	2.82
Molybdenum	32.12	15.36	0.726	171.8	295.7	0.626	2214	1.08	3.28
Zirconium	27.43	0.756	0.623	20.5	0.088	0.900	10061	1.20	3.46
Tantalum	28.57	0.809	0.696	41.9	1.392	0.698	4265	1.45	3.81
Niobium	26.75	0.789	0.656	40,76	1.293	0.535	3657	1.23	2.95

Table 6. Values of the elements of the equivalent circuit R(QR(QR)) for pure metals in Ringer's solution

Alloy	R_s Ohm.cm^2	CPE1 $10^4.Q_{pas}$ S.s^n/cm^2	n_1	R_{pas} Ohm.cm^2	CPE2 $10^4.Q_{dl}$ S.s^n/cm^2	n_2	R_{ct} Ohm.cm^2	$10^3.\chi^2$	ε
Titanium	26.86	1.261	0.638	13.4	0.195	0.757	13790	7.96	2.82
Molybdenum	31.97	1.709	0.720	192	234.1	0.633	2318	1.26	3.55
Zirconium	26.78	0.625	0.572	19.0	0.116	0.892	15610	1.28	3.58
Tantalum	28.57	0.809	0.696	84.5	0.344	0.712	8390	1.47	3.83
Niobium	26.25	0.673	0.593	79.3	0.325	0.532	7245	1.30	3.75

Table 7. Ringer Values of the elements of the equivalent circuit R(QR)(QR) for pure metals in Ringer's solution

Alloy	R_s Ohm.cm^2	CPE1 $10^4.Q_{pas}$ S.s^n/cm^2	n_1	R_{pas} Ohm.cm^2	CPE2 $10^4.Q_{dl}$ S.s^n/cm^2	n_2	R_{ct} Ohm.cm^2	$10^3.\chi^2$	ε (%)
Titanium	27.90	2.533	0.679	14,5	0.048	0.988	12820	0.76	2.76
Molybdenum	31.64	7.341	0.807	818	810	0.554	3697	1.08	3.28
Tantalum	27.78	1.250	0.898	174	1.169	0.656	8418	1.19	3.45
Zirconium	27.23	0.832	0.708	196	1.154	0.977	9823	1.89	4.35
Niobium	24.32	0.756	0.676	180	1.156	0.867	5892	1.23	3.31

Overall, the correlation of the instantaneous and stimulated corrosion parameters (Tables 3 and 4) with the impedance parameters and equivalent circuit models (Tables 5-7) demonstrates that Ti and Ta are the main promoters of corrosion resistance in multicomponent systems, while Mo and Nb should be used together with them to benefit from phase stabilization and mechanical properties without compromising electrochemical performance.

These findings justify the proposed alloy compositions, in which the passivation role of Ti and Ta compensates for the susceptibility of Mo and Nb, and Zr contributes to biocompatibility, thus ensuring the optimal balance between mechanical strength and electrochemical behavior in physiological environments [25-28].

The instantaneous corrosion parameters determined for the Ti–Mo–Zr–Ta–Nb alloys in Ringer's solution are summarized in Table 8. These values provide a comparative picture of the corrosion potential, polarization resistance, and corrosion rate, highlighting the influence of niobium content on the electrochemical stability of the alloys.

Table 8. Instantaneous corrosion parameters for Ti–Mo–Zr–Ta–Nb alloys in Ringer's solution

Alloy	E_{cor} [mV]	R_p [kohm.cm^2]	J_{cor} [mA/cm^2]	v_{cor} [mm/an]	b_a [mV/dec.]	b_c [mV/dec.]
Ti20Mo7Zr15Ta5Nb	-104	15.76	2.233	19.40	240	-186
Ti20Mo7Zr15Ta7Nb	-128	5.63	4.685	42.27	175	-143
Ti20Mo7Zr15Ta10Nb	-114	2.82	10.911	94.58	221	-134
Ti20Mo7Zr15Ta15Nb	-340	12.93	1.739	15.07	134	-144

It can be observed that the alloy with the highest niobium content (Ti20Mo7Zr15Ta15Nb) exhibits the most negative corrosion potential but also the lowest corrosion current density and corrosion rate, confirming its superior passivation capacity. In contrast, intermediate Nb contents (7–10%) lead to higher corrosion currents and reduced polarization resistance, indicating less stable electrochemical behavior [21-22].

Conclusions

The results obtained in this work highlight the major role of the chemical composition and structure of the passive layer in determining the corrosion behavior of titanium-based alloys intended for biomedical applications. The study of pure metals has shown that titanium and tantalum rapidly develop stable protective films (TiO_2 and Ta_2O_5), which gives them good corrosion resistance and a pronounced passivating character. Zirconium presents limited passivation, with porous films, while molybdenum is prone to generalized corrosion, without effective protection, which confirms its vulnerability in environments similar to physiological ones.

The production of Ti–Mo–Zr–Ta–Nb alloys was based on criteria of biocompatibility and structural stability, but their processing raises major technological difficulties, generated by the high melting temperatures and the reactivity of liquid titanium with contact materials. The use of modern methods, such as vacuum melting or additive processing by selective laser melting (SLM), may represent viable solutions for the fabrication of complex implants with advanced control of composition and microstructure.

In the perspective of future developments, optimization directions could include: adjusting the proportions of alloying elements to maximize the synergy between passivity and mechanical strength; using thermal and thermomechanical treatments to stabilize the desired phases; as well as applying surface treatments (controlled oxidation, bioactive coatings) to increase corrosion resistance and integration into the biological environment. The integration of these strategies could lead to the development of advanced biomaterials, capable of meeting stringent clinical requirements related to durability, safety and long-term performance.

Acknowledgement

This work was supported by BIO-SIMTIT Grant of the Ministry of Research, Innovation and Digitization, CCCDI – UEFISCDI, project number PN-IV-P7-7.1-PED-2024-0080, within PNCDI IV and also was supported by a grant of the Ministry of Research, Innovation and Digitization, CNCS/CCCDI - UEFISCDI, project number ERANET-ERAMIN-3-Cool&SmartTit-1, contract no 8/2024 within PNCDI IV.

References

[1] M. Sarraf, E.R. Ghomi, S. Alipour, S. Ramakrishna, N.L. Suikman, *A state-of-the-art review of the fabrication and characteristics of titanium and its alloys for biomedical applications*, **Bio-Design and Manufacturing**, **5**, 2021, pp. 371–395. https://doi.org/10.1007/s42242-021-00170-3

[2] C. Veiga, J.P. Davim, A. Loureiro, *Properties and applications of titanium alloys: A brief review*, **Reviews on Advanced Materials Science**, **32**, 2012, pp. 133–148.

[3] P. Pushp, D. Mabrukar, C. Arati, *Classification and applications of titanium and its alloys*, **Materials Today: Proceedings**, **54**, 2022. https://doi.org/10.1016/j.matpr.2022.01.008

[4] J. Willis, S. Li, S.J. Crean, F.N. Barrak, *Is titanium alloy Ti-6Al-4V cytotoxic to gingival fibroblasts—A systematic review*, **Clinical and Experimental Dental Research**, **7(6)**, 2021, pp. 1037–1044. https://doi.org/10.1002/cre2.444

[5] E. Marin, A. Lanzutti, *Biomedical applications of titanium alloys: A comprehensive review*, **Materials**, **17**, 2024, 114.

[6] M. S.Baltatu, P. Vizureanu, A.V. Sandu, I. Baltatu, D.D. Burduhos-Nergis, M. Benchea. *Prospects on titanium biomaterials*. **European Journal of Materials Science and Engineering, 8(4)**, 2023, 191–200. Retrieved from https://ejmse.ro/articles/08_04_01_EJMSE-23-191.pdf

[7] A. Savin, P. Vizureanu, Z. Prevorovsky, M. Chlada, J. Krofta, M.S. Baltatu, B. Istrate, R. Steigmann, *Noninvasive evaluation of special alloys for prostheses using complementary methods*, **IOP Conference Series: Materials Science and Engineering**, **374**, 2018, 012030.

[8] I. Baltatu, L. Benea, P. Vizureanu, M.S. Baltatu, M. Nabialek. *Biofunctionalization of titanium alloys: Methods and applications*. **European Journal of Materials Science and Engineering**, **8(4)**, 2023, 218–229. Retrieved from https://ejmse.ro/articles/08_04_05_EJMSE-23-218.pdf

[9] R.R. Boyer, R.D. Briggs, *The Use of β Titanium Alloys in the Aerospace Industry*, **Journal of Materials Engineering and Performance**, **14**, 2005, pp. 681–685.

[10] I. Baltatu, P. Vizureanu, M.S. Baltatu, D. Achitei, M. Nabialek. *Structural analysis of Ti–Mo alloys*. **European Journal of Materials Science and Engineering, 4(1)**, 2019, 63–70. Retrieved from https://ejmse.ro/articles/EJMSE_04_01_06_Baltatu.pdf

[11] M.S. Baltatu, P. Vizureanu, A.V. Sandu, C. Solcan, L.D. Hritcu, M.C. Spataru, *Research Progress of Titanium-Based Alloys for Medical Devices*, **Biomedicines**, **11**, 2023, 2997.

[12] M. Najafizadeh, S. Yazdi, M. Bozorg, M. Ghasempour-Mouziraji, M. Hosseinzadeh, M. Zarrabian, P. Cavaliere, *Classification and applications of titanium and its alloys: A review*, **Journal of Alloys and Compounds Communications**, **3**, 2024, 100019. https://doi.org/10.1016/j.jacomc.2024.100019

[13] M.S. Bălţatu, P. Vizureanu, V. Geantă, C. Nejneru, C.A. Ţugui, S.C. Focşăneanu, *Obtaining and Mechanical Properties of Ti-Mo-Zr-Ta Alloys*, **IOP Conference Series: Materials Science and Engineering**, **209**, 2017, 012019.

[14] A. Martinez, K. Osen, E. Skybakmoen, O. Kjos, G.M. Haarberg, K. Dring, *New method for low-cost titanium production*, **Key Engineering Materials**, **436**, 2010, pp. 41–53.

[15] K.K. Wong, H.C. Hsu, S.C. Wu, W.F. Ho, *A Review: Design from Beta Titanium Alloys to Medium-Entropy Alloys for Biomedical Applications*, **Materials**, **16(21)**, 2023. https://doi.org/10.3390/ma16217046

[16] Y. Zhang, Y. Ma, *Research Progress on Titanium–Niobium Micro-Alloyed High-Strength Steel*, **Materials**, **18(2)**, 2025. https://doi.org/10.3390/ma18020325

[17] M. Zhong, Y. Lin, *Area effect during the fracture process of high-Niobium-Titanium-Aluminum alloys under continuous tension loading-unloading*, **Frontiers in Materials**, 2023. https://doi.org/10.3389/fmats.2023.1214872

[18] C. Jiménez-Marcos, J.C. Mirza-Rosca, M.S. Baltatu, P. Vizureanu, *Preliminary studies of new heat-treated titanium alloys for use in medical equipment*, **Results in Engineering**, **25**, 2025, 104477. https://doi.org/10.1016/j.rineng.2025.104477

[19] C. Jiménez-Marcos, J.C. Mirza-Rosca, M.S. Baltatu, P. Vizureanu, *Two novel Ti–Mo–Ta–Zr alloys for medical devices: Their microstructure, corrosion resistance and microhardness characteristics*, **Materials Chemistry and Physics**, **334**, 2025, 130511. https://doi.org/10.1016/j.matchemphys.2025.130511

[20] E.M. Safwat, S.A. Abdel-Gawad, M.A. Shoeib, *Electrochemical anodization of cast titanium alloys in oxalic acid for biomedical applications*, **Frontiers of Chemical Science and Engineering**, **18(2)**, 2024. https://doi.org/10.1007/s11705-023-2368-y

[21] V.O. Semin, A.P. Chernova, A.V. Erkovich, *Electrochemical Properties and Structure of the TiNi Alloy Surface Layers Implanted with Titanium and Niobium Ions*, **Inorganic Materials: Applied Research**, **15**, 2024, pp. 638–648. https://doi.org/10.1134/S2075113324700060

[22] G. Senopati, R.A.R. Rashid, I. Kartika, S. Palanisamy, *Recent Development of Low-Cost β-Ti Alloys for Biomedical Applications: A Review*, **Metals**, **13(2)**, 2023. https://doi.org/10.3390/met13020194

[23] A. Li, Q. Wang, R. Chen, X. Din, Y. Su, H. Fu, *Application of alloying for enhancing the corrosion resistance of titanium alloys: A review*, **Materials Today Communications**, **42**, 2025. https://doi.org/10.1016/j.mtcomm.2024.111111

[24] M.M. Iancu, C.I. Tatia, A. Robu, M.L. Vasilescu, I. Antoniac, A.M. Fratila. *Current trends on materials and methods for teeth whitening*, **European Journal of Materials Science and Engineering, 9(4)**, 2024, pp. 323-336, DOI: 10.36868/ejmse.2024.09.04.323

[25] A.N. Omran, M.M. Ali, M.M. Kh, *Biocompatibility, corrosion, and wear resistance of β titanium alloys for biomedical applications*, **Applied Physics A**, **126(942)**, 2020. https://doi.org/10.1007/s00339-020-04118-9

[26] T.M. Sridhar, S. Vinodhini, U. Kamachi, B. Venkatachalapathy, R. Kulandaivelu, *Load-bearing metallic implants: electrochemical characterisation of corrosion phenomena*, **Materials Technology**, **31**, 2016, pp. 1–14. https://doi.org/10.1080/10667857.2016.1220752

[27] H. Jaber, J. Kónya, P. Pinke, L. Toth, T. A. Kovács. *Investigating the impact of annealing temperature on the microstructure and mechanical performance of selectively laser melted Ti6Al4V alloy.* **European Journal of Materials Science and Engineering, 8(4)**, 2023, 216–225. Retrieved from https://ejmse.ro/articles/08_04_06_EJMSE-23-216.pdf

[28] V. M. Tabie, J. K. Quaisie, J. Li, P. Yamba, X. Xu. *The influence of ceramic particles on corrosion behavior of Ti750 alloy composites*. **European Journal of Materials Science and Engineering, 8(2)**, 2022, 187–195. Retrieved from https://ejmse.ro/articles/08_02_02_EJMSE-22-187.pdf

Received: June 26, 2025
Accepted: September 05, 2025